Vibrationally resolved O 1*s* core-excitation spectra of CO and NO

R. Püttner,[1,*] I. Dominguez,[2] T. J. Morgan,[3] C. Cisneros,[4] R. F. Fink,[5] E. Rotenberg,[2] T. Warwick,[2] M. Domke,[1] G. Kaindl,[1] and A. S. Schlachter[2]

[1]*Institut für Experimentalphysik, Freie Universität Berlin, Arnimallee 14, D-14195 Berlin-Dahlem, Germany*

[2]*Lawrence Berkeley National Laboratory, 1 Cyclotron Road, Berkeley, California 94720*

[3]*Department of Physics, Wesleyan University, Middletown, Connecticut 06459*

[4]*Instituto de Fisica, Apartado Postal 139-B, Cuernavaca 62191, Mexico*

[5]*Lehrstuhl für Theoretische Chemie, Ruhr-Universität Bochum, D-44780 Bochum, Germany*

(Received 16 December 1998)

High-resolution photoabsorption spectra of CO and NO below the O 1*s* ionization threshold are presented. The vibrational fine structure of the O $1s\rightarrow\pi^*$ and O $1s^{-1}$ Rydberg excitations could be resolved for both molecules, allowing a determination of the vibrational energies and intramolecular distances of the core-excitation states in CO and NO from Franck-Condon analyses. *Ab initio* calculations are performed for the O $1s\rightarrow\pi^*$ excitation in CO to give an independent confirmation of the spectroscopic parameters derived from the Franck-Condon analysis. The spectral features of the O $1s^{-1}$ Rydberg region in CO are reassigned on the basis of the experimental results. The results obtained for the O $1s^{-1}3s$ Rydberg state in NO support the idea of a weakening of the molecular bond upon an O $1s^{-1}$ ionization process. [S1050-2947(99)06205-8]

PACS number(s): 33.20.Rm, 33.20.Tp, 33.15.Dj, 33.15.Ry

I. INTRODUCTION

Measurements of medium-resolution photoemission spectra of core-ionized molecules in the 1970s revealed an asymmetric line shape, indicating the presence of vibrational fine structure [1]. These experimental findings stimulated a large number of theoretical investigations on the potential-energy surfaces of C, N, and O $1s^{-1}$ core-ionized states of small molecules [2–5], and resulted in the conclusion that C 1*s*/N 1*s* (*O* 1*s*) core ionization leads to a strengthening (weakening) of the molecular bond [6]. These effects on the molecular bond are also expected for core-to-Rydberg excitations according to their similar valence-electron distribution.

Recent improvements in synchrotron light sources and beamlines have made it possible to resolve the vibrational fine structure of numerous core-excited molecules using photon energies up to $h\nu\cong 400$ eV. Extensive studies have been performed using photoabsorption and photoemission spectroscopy to obtain information about the potential-energy surfaces of core-excited molecules; see, e.g., Si $2p^{-1}$ in SiX_4 (X=H,D,F,CH_3,Cl,Br) [7], C $1s^{-1}$ in CO [8,9] and CH_4 [10,11], and N $1s^{-1}$ in NO [12], and references therein. These measurements confirmed the predicted strengthening of the molecular bond, i.e., an increase of the vibrational energy and a decrease of the equilibrium distance upon ionization/excitation for C $1s^{-1}$ and N $1s^{-1}$ core-ionized states as well as the corresponding Rydberg excitations. However, at even higher energies, the instrumental resolution achieved with photon (photoabsorption and photoemission spectroscopy) and electron [electron-energy-loss spectroscopy (EELS)] excitation was not sufficient until recently to obtain complete information on the vibrational fine structure. Therefore, a number of earlier measurements below the O 1*s* ionization threshold were not able to resolve the vibrational fine structure of CO [13,14] and NO [15,16]. Only recent experiments were able to obtain partial information about the vibrational fine structure of O $1s^{-1}$ core-excited and core-ionized states of NO [12] and CO [8,17]. These recent photoabsorption [8] and photoemission [17] spectra of CO exhibited an increase of the equilibrium distance and a decrease of the vibrational energy, i.e., a weakening of the bond and, therefore, gave a first support of the theoretical predictions.

Here we report on photoabsorption measurements of CO and NO below the O 1*s* ionization threshold with substantially improved resolution ($\Delta E\cong 65$ meV), compared to recent measurements performed at the SX700/II monochromator at BESSY in Berlin, Germany with a resolution of $\Delta E\cong 120$ meV [8,12]. This improved resolution results in completely resolved vibrational fine structures, and allows Franck-Condon analysis of the spectra, providing information on the potential-energy surfaces of the core-excited states. To compare the experimental results derived for the O $1s\rightarrow\pi^*$ excitations in both molecules, accurate *ab initio* calculations for CO similar to those published earlier for NO [19] were performed, and good agreement was obtained. On the basis of the Franck-Condon analysis a reassignment of the Rydberg region in CO is given. The vibrational fine structure of the lowest Rydberg state in NO reveals a lower vibrational energy and a larger equilibrium distance compared to the ground state, supporting the general conclusion of Ref. [6] of a weakening of the molecular bond upon O 1*s* core ionization.

*Present address: Department of Physical Sciences, University of Oulu, Linnanmaa, 90570 Oulu, Finland.

II. EXPERIMENTAL AND DATA ANALYSIS

The measurements were performed at the 7.0.1 undulator beamline of the Advanced Light Source in Berkeley, California, which is equipped with a spherical-grating monochromator. The built-in photoionization cell consisting of two parallel plates with an active length of 20 cm for collecting the charged particles was used. The photoionization cell was separated from the UHV of the monochromator by a 1000-Å-thick Al (1% Si) window; it was filled with 10 to 50 μbar of CO or NO. The spectra were measured with the 925 lines/mm grating using 8-μm entrance and exit slits, resulting in a spectral resolution of $\Delta E \cong 65$ meV.

Two calibration points are necessary for an exact calibration of a spherical-grating monochromator. For the energy range of the grating used, no high-accuracy energy values for calibration are available. Therefore, the present spectra were calibrated in a linear way to the value of the O $1s^{-1}3s\sigma$ Rydberg state for NO given by Remmers *et al.* [12]. The energy of the largest photoionization yield of the O $1s^{-1}\pi^*$ excitation in CO obtained in this way agrees within the error bars with the EELS values of 534.21(8) eV achieved by Sodhi and Brion [18]. The absolute error bars in energy are estimated to be ± 50 meV on the basis of the described calibration; the relative error bars are distinctly smaller (about ± 10 meV), and are given in the tables.

The spectral features were described with Voigt profiles in the least-squares fit analyses, i.e., with Lorentzians convoluted by a Gaussian, to simulate the spectrometer function. The linewidth of the Gaussian was used as a free parameter in the fit procedure of all spectra, yielding a spectral resolution of $\Delta E = 65 \pm 10$ meV.

The potential-energy surfaces of a nondissociative molecular state can be described with a Morse potential, which is characterized by the equilibrium distance r, the vibrational energy $\hbar\omega$, and the anharmonicity $x\hbar\omega$. In this paper double and single primes denote the values of r, $\hbar\omega$, and $x\hbar\omega$ for the ground and core-excited states, respectively. To obtain information about the values r', $\hbar\omega'$, and $x\hbar\omega'$ of the core-excited states, Franck-Condon analyses were performed. In these analyses the intensity distribution of the vibrational substates of the core-excited states are calculated by using the overlap of the vibrational wave function of the ground and core-excited states. For this purpose, the vibrational wave functions of the ground state are calculated on the basis of r'', $\hbar\omega''$, and $x\hbar\omega''$; these values are taken from the literature [20]. The vibrational wave functions of the core-excited states are calculated by varying of the fit parameters r', $\hbar\omega'$, and $x\hbar\omega'$.

Two different algorithms were used to calculate the vibrational wave functions and the intensity distributions of the vibrational substates of the core-excited state: The Franck-Condon analyses of the Rydberg states in CO and NO are performed with the simple and fast algorithm of Hutchisson [21,22]. However, this considers only the terms $(R-r)^2$ and $(R-r)^3$ in the development of the potential-energy surface $V(R)$, with R being the internuclear distance; it underestimates the intensity of the higher vibrational substates [23]. It turned out that this approximation was not sufficient to describe the O $1s \rightarrow \pi^*$ excitations, which reveal a large number of vibrational substates. The latter states were fitted with an algorithm that is based on the publications of Halman and Laulich [24] and Ref. [25]; it uses the complete Morse potential to calculate the vibrational substates and leads to highly improved fit results.

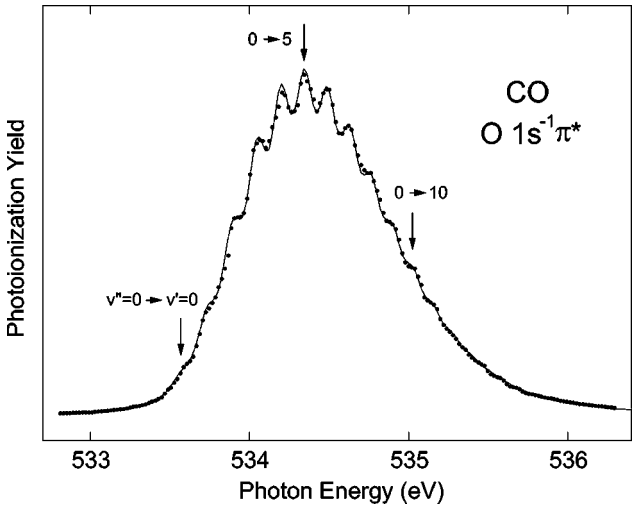

FIG. 1. O $1s^{-1}\pi^*$ excitation in CO. The solid line through the data points represents the results of a Franck-Condon analysis.

III. CO O 1*s* EXCITATIONS

A. Valence region

The photoionization spectrum of the O $1s^{-1}\pi^*$ excitation in CO, with completely resolved vibrational fine structure, is shown in Fig. 1. This improved spectrum allowed a Franck-Condon analysis of this excitation, resulting in an increase of the equilibrium distance from $r'' = 1.1283$ Å in the electronic ground state to $r' = 1.291(3)$ Å in the core-excited state. In addition, a decrease of the vibrational energy from $\hbar\omega'' = 269.025$ meV in the ground state to $\hbar\omega' = 166(1)$ meV in the core-excited state as well as a slight increase of the anharmonicity from $x\hbar\omega'' = 1.647$ meV to $x\hbar\omega' = 1.8(1)$ meV were derived. We obtain a decrease of the dissociation energy from $D_e'' = 11.0$ eV in the ground state to $D_e' = 3.9$ eV in the core-excited state according to $D_e = (\hbar\omega)^2/4x\hbar\omega$. The resulting parameters of the core-excited state agree fairly well with calculations of Correia *et al.* [26], with $\hbar\omega' = 176.8$ meV, $x\hbar\omega' = 2.3$ meV, and $r' = 1.280$ Å. The parameters agree also very well with the values of the $Z+1$ molecule CF, with $\hbar\omega' = 162$ meV, $x\hbar\omega' = 1.4$ meV, and $r' = 1.2718$ Å [20]. The increase of the equilibrium distance as well as the decrease of the vibrational energy and the dissociation energy upon excitation can readily be understood on the basis of an excitation into an antibonding π^* orbital. In addition to the above results, the lifetime width of the O $1s^{-1}\pi^*$ excitation was determined to be 143(5) meV.

Ab initio calculations similar to the approach described in Ref. [19] were performed for the spectroscopic parameters r, $\hbar\omega$, and $x\hbar\omega$ in order to check the reliability of the experimental values of the parameters for the O $1s^{-1}\pi^*$ excited state of CO. For the carbon atom we employed the $11s7p/9s7p$ basis set of Huzinaga [27], augmented by one p set (exponent 28.0), four d sets (exponents 20.0, 1.848, 0.649, and 0.228) and two f sets (exponents 1.419 and

TABLE I. Calculated and experimental spectroscopic parameters for the ground state, the C $1s^{-1}\pi^*$ and O $1s^{-1}\pi^*$ core-excited state of CO. Given are the energies E, the equilibrium distances r, the vibrational energies $\hbar\omega$, and the anharmonicities $x\hbar\omega$. For the energy E of the O $1s^{-1}\pi^*$ excitation, the absolute error is given.

	CO ($X^1\Sigma^+$)		CO (C $1s^{-1}\pi^*$ $^2\Pi$)		CO (O $1s^{-1}\pi^*$ $^2\Pi$)	
State	calc.	expt.	calc.	expt.	calc.	expt.
E (eV)			287.61	287.41[a]	533.48	533.57(5)[b]
r (Å)	1.1298	1.1283[c]	1.1555	1.1529[d]	1.2874	1.291(3)[b]
$\hbar\omega$ (meV)	259.39	269.02[c]	249	258[d]	161	166(1)[b]
$x\hbar\omega$ (meV)	1.386	1.647[c]	1.6	1.9[d]	1.5	1.8(1)[b]

[a]Reference [29].
[b]This work.
[c]Reference [20].
[d]Reference [30].

0.485). The basis set used for the oxygen atom was given in Ref. [19], and contains the same number of basis functions as for the carbon atom. This rather large and strongly decontracted basis set allows us to describe the relaxation of the core orbitals and the correlation energy of both the core and valence orbitals. As in the preceding work of Fink on the core excited states of NO [19], all energies were calculated with the multi configuration reference coupled electron pair approach (MCCEPA) [28] using reference wave functions from complete active space self-consistent-field calculations with active spaces including the 1π (π) and 2π (π^*) orbitals. The core orbital was included additionally in the active space for the core-excited states. Throughout, excitations from all occupied orbitals were included in the MCCEPA configuration space.

The calculations were performed for the ground state, the C $1s^{-1}\pi^*$ and O $1s^{-1}\pi^*$ excited states of CO at different geometries between 0.9 and 2.1 Å . The resulting potential-energy surfaces were used to obtain the excitation energies E (including the zero-point vibration), the equilibrium distances r, the vibrational energies $\hbar\omega$, and the anharmonicities $x\hbar\omega$. The theoretical and experimental results are summarized in Table I. The excitation energies agree to within 0.2 eV, the equilibrium distances deviate by less than 0.005 Å, the theoretical calculated vibrational energies are underestimated by less than 4%, and the calculated values for the anharmonicity are generally $\cong 0.3$ meV too small. The deviations are due to the particular choice of the wave functions and possibly also to relativistic effects. Altogether, the theoretical results given in the present paper agree better with the experimental results than earlier calculations [26], and show the same quality as the calculations performed in Ref. [19] for NO (see below). The good agreement, especially for the ground state and the O $1s^{-1}\pi^*$ core-excited state, confirm the calculations and the validity of the fitting procedure performed.

B. Rydberg region

The Rydberg region of the O 1s core-excitation spectrum of CO is shown in Fig. 2 together with the assignment. For the two lowest Rydberg states at $h\nu \cong 539$ (O $1s^{-1}3s\sigma$) and 540 eV (O $1s^{-1}3p\pi$), Franck-Condon analyses has been performed, resulting in different values for the equilibrium distance (see below). The equilibrium distance of the O $1s^{-1}3p\pi$ state was transferred to the higher Rydberg states to describe their line shapes in the fit analysis of the complete spectrum. The result of this fit analysis is presented by the solid line through the data points of Fig. 2. The derived energy positions of the resonances, together with the quantum defects δ and the assignment, are given in Table II. For comparison, the energy positions and quantum defects calculated by in Ref. [31] are also given. By presupposing the $nl\pi$ states to be more intense then the $nl\sigma$ states, which is in agreement with calculations in Ref. [31] and by Padial *et al.* [32], there remains only one small uncertainty in the assignment. The assumption of constant quantum defects for the Rydberg series leads to the assignment O $1s^{-1}4s\sigma$ for the resonance at 540.980 eV with a quantum defect $\delta = 1.05$ ($\delta = 1.06$ for O $1s^{-1}3s\sigma$). As a consequence, the resonance at 540.777 eV has to be assigned to O $1s^{-1}3d\sigma$. However, calculations in Ref. [31] predicted an increase of the quantum defect for the s series from $\delta = 1.07$ for O $1s^{-1}3s\sigma$ to $\delta = 1.18$ for O $1s^{-1}4s\sigma$ state (see also Table

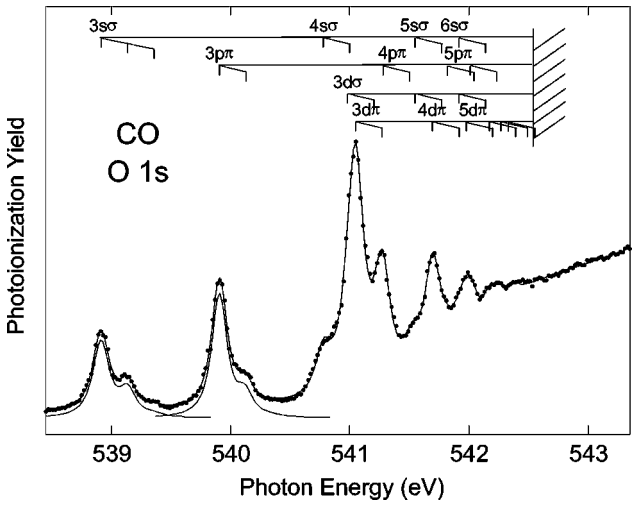

FIG. 2. Rydberg region of CO below the O 1s ionization threshold. The solid line through the data points represents the results of a fit analysis. The subspectra below the spectrum represent the results of a Franck-Condon analysis of the Rydberg states O $1s^{-1}3s\sigma$ and O $1s^{-1}3p\pi$. The assignment is given by the vertical bar diagrams above the spectrum. The first bar for each resonance represents the $v''=0 \rightarrow v'=0$ excitation, while the other bars represent higher vibrational substates.

TABLE II. The energies E and quantum defects δ of the Rydberg states in CO below the O $1s$ ionization threshold, as obtained from the fit analysis. The relative errors for the energies are estimated to ± 10 meV. For comparison, the theoretical results of Ref. [31] are also given. For the values in brackets see text.

	This work		Ref. [31]	
	E (eV)	δ	E (eV)	δ
$3s\sigma$	538.912	1.06	538.910	1.07
$4s\sigma$ $(3d\sigma)$	540.777	1.22(0.22)	540.829(541.101)	1.18(−0.07)
$5s\sigma$	541.547	1.30		
$6s\sigma$	541.961	1.34		
$3p\sigma$			540.175	0.61
$3p\pi$	539.906	0.73	540.012	0.68
$4p\pi$	541.279	0.72	541.318	0.67
$5p\pi$	541.819	0.67		
$6p\pi$	542.009	0.95		
$3d\sigma$ $(4s\sigma)$	540.980	0.05(1.05)	541.101(540.829)	−0.07(1.18)
$4d\sigma$	541.547	0.30	541.727	−0.09
$5d\sigma$	541.961	0.34		
$3d\pi$	541.049	−0.02	541.074	−0.04
$4d\pi$	541.694	0.00	541.714	−0.05
$5d\pi$	541.976	0.10		
$6d\pi$	542.170	−0.04		
$7d\pi$	542.266	−0.01		
$8d\pi$	542.329	0.02		
I_p	542.543			

II). A similar increase of the quantum defect was calculated for NO by Kosugi *et al.* [16], in agreement with the experimental findings of Remmers *et al.* [12] and the results of the present work (see below). On the basis of the arguments given supported by our calculations (see below), the assignment O $1s^{-1}4s\sigma$ for the resonance at 540.777 eV and O $1s^{-1}3d\sigma$ for the resonance at 540.980 eV is preferred. This does not influence the assignment of the higher Rydberg states, since the splitting of the $nd\sigma$ and $(n+1)s\sigma$ states cannot be resolved for $n \geqslant 3$.

Furthermore, for $n \geqslant 3$ the $nd\sigma$ and $(n+1)s\sigma$ orbitals are generally strongly mixed in linear molecules. This has, e.g., been observed experimentally [33] and theoretically [34] for the Rydberg orbitals of the $\pi^* \rightarrow$Rydberg excited NO. These states of NO are isovalence-electronic to O $1s^{-1}$ core-excited CO. A partial-wave analysis of the $(n+1)s\sigma$ and $nd\sigma$ Rydberg orbitals in valence-excited NO showed only $\cong 62\%$ s and d character for their respective cases [34]. We performed a detailed theoretical analysis similar to that given by Kaufmann [34], and found the mixing of the $(n+1)s\sigma$ and $nd\sigma$ Rydberg orbitals is even larger for the O $1s$ core-excited states in CO, i.e., the contribution of the dominant character is only about 55%. The partial-wave analysis for the Rydberg state at 540.777 eV $(4s\sigma)$ resulted in 50% s character, 4% p character, and 46% d character; and for the Rydberg state at 540.980 eV $(3d\sigma)$ resulted in 46% s character, 1% p character, and 54% d character. These results support the assignment given above based on the convention of labeling states according to their dominant partial-wave contribution. These results indicate as well that, in the case given, the assignment in terms of $ns\sigma$ or $nd\sigma$ is only of minor significance.

The assignment presented leads to good agreement with the energies and intensities of theoretical results given in

TABLE III. The results of the Franck-Condon analyses for the O $1s^{-1}3s\sigma$ and O $1s^{-1}3p\pi$ states in CO. For comparison, the results of Domke *et al.* [8] and the values for the $Z+1$ molecule CF [20] are also given. The vibrational energies of the molecule CF are multiplied with $\sqrt{1.0725}$ according to the different reduced masses.

	Ground state		This work		Domke *et al.*		CF	
	r'' (Å)	$\hbar\omega''$ (meV)	r' (Å)	$\hbar\omega'$ (meV)	r' (Å)	$\hbar\omega'$ (meV)	r' (Å)	$\hbar\omega'$ (meV)
	1.12832	269.025						
$3s\sigma$			1.169(2)	223(3)	1.167(9)	227(8)	1.154	229
$3p\pi$			1.158(2)	223(3)	1.159(9)	224(9)	1.151	232

TABLE IV. Electronic configurations and molecular states of NO in the electronic ground state, in O $1s^{-1} \equiv 1\sigma^{-1}$ core-excited states, and O $1s^{-1}$ core-ionized states (adapted from Ref. [15]). The numbers in parentheses refer to the numbers of states of this symmetry. $n\sigma$ and $n\pi$ denote Rydberg orbitals with σ and π symmetries, respectively.

	Electronic configuration									
	1σ	2σ	3σ	4σ	1π	5σ	2π	$n\sigma$	$n\pi$	Molecular state
NO	2	2	2	2	4	2	1			$X^2\Pi$
NO^{K*}	1	2	2	2	4	2	2			$^4\Sigma^-$, $^2\Sigma^-$, $^2\Delta$, $^2\Sigma^+$
NO^{K*}	1	2	2	2	4	2	1	1		$^4\Pi$, $^2\Pi$, $^2\Pi$
NO^{K*}	1	2	2	2	4	2	1		1	$^4\Sigma^-$, $^4\Delta$, $^4\Sigma^+$, $^2\Sigma^-(2)$, $^2\Delta(2)$, $^2\Sigma^+(2)$
NO^{K+}	1	2	2	2	4	2	1			$^3\Pi$, $^1\Pi$

Ref. [31]. The main difference between experiment and theory is an inversion of the orbital order of the *nd* states due to the small $nd\sigma$-$nd\pi$ splitting: $3d\sigma$-$3d\pi$ (expt.) = 69 meV and $3d\sigma$-$3d\pi$ (theor.) = −27 meV.

However, the assignment obtained in this work differs from the results given by Domke *et al.* [8], in which it was assumed that the $np\pi$ series was the most intense. This is in contradiction to the latest theoretical results [31], and leads to the doubtful intensity ratio of the O $1s^{-1}3p\pi$ and O $1s^{-1}4p\pi$ states; therefore, their assignment has to be rejected.

The results of the Franck-Condon analysis of the O $1s^{-1}3s\sigma$ and O $1s^{-1}3p\pi$ states are summarized in Table III. For comparison, the results of Domke *et al.* [8] and the values of the $Z+1$ molecule CF are also given, showing good agreement. From the different intensity distribution for the vibrational substates of these states, as seen in Fig. 2, we estimate from Franck-Condon analysis that the change of the equilibrium distances is larger by approximately 25% for the O $1s^{-1}3s\sigma$ state. We conclude that the lowest Rydberg state is a mixed state, i.e., a Rydberg state with some valence character. Valence contributions for the lowest Rydberg state were observed previously in SiF_4 [35] and SiH_4/SiD_4 [36].

Although the equilibrium distances in the O $1s^{-1}3s\sigma$ and O $1s^{-1}3p\pi$ states clearly differ, differences in the vibrational energy were not observed. This is in contradiction to the expectation that a larger change in the equilibrium distance upon excitation results in a larger change of the vibrational energy. The deviation from the expected results can be explained with the calculations in Ref. [31]; they predicted a small contribution of the O $1s^{-1}3p\sigma$ state to the spectrum, which may influence the energy region between the $v'=0$ and 1 vibrational substates of the O $1s^{-1}3p\pi$ state. In accordance with its small predicted intensity, the O $1s^{-1}3p\sigma$ state is not resolved; however, its possible presence in the spectrum may cause a slightly incorrect value for the vibrational energy of the O $1s^{-1}3p\pi$ state.

An increase of the equilibrium distance and a decrease of the vibrational energy is found, in agreement with Domke *et al.* [8] and Kempgens *et al.* [17] for the O $1s^{-1}$ Rydberg states in CO. A lifetime width for the Rydberg states of 135(8) meV was observed.

IV. NO O 1s EXCITATIONS

A. Open-shell molecules

NO has one additional electron compared to CO, which is located in the antibonding π^* orbital. Due to the single occupancy of the π^* orbital in its electronic ground state, NO is an open-shell molecule. Upon core excitation, the single π^* electron can interact with the core hole and the excited electron, leading to new effects as compared to CO. The final-state symmetries resulting from the interaction of the electrons in the partially filled orbitals are summarized in Table IV. Note that a pure molecular assignment of the orbitals is used in Table IV, i.e., the O 1s (π^*) orbital is described with 1σ (2π). Certain states can be observed on the basis of spin-selection rules: the doublet states for photoabsorption ($\Delta S=0$), and the singlet and triplet states for photoemission ($\Delta S=\pm\frac{1}{2}$). Thus, e.g., three out of the four O $1s^2\pi^* \rightarrow O1s^1(\pi^*)^2$ excitations and two O $1s^{-1}$ ionization thresholds are allowed and expected to contribute to the spectrum. A more detailed discussion of the interaction between the electrons in the partially filled orbitals and its influence on the spectral features is given by Wight and Brion [15] and Kosugi *et al.* [16].

B. Valence region

Figure 3 shows the O $1s^2\pi^* \rightarrow O1s\pi^{*2}$ excitations in NO, including the three different electronic states due to the interaction between the core hole and the two π^* electrons. The assignment of the states is adopted from the calculations performed by Kosugi *et al.* [16], Wight and Brion [15], and

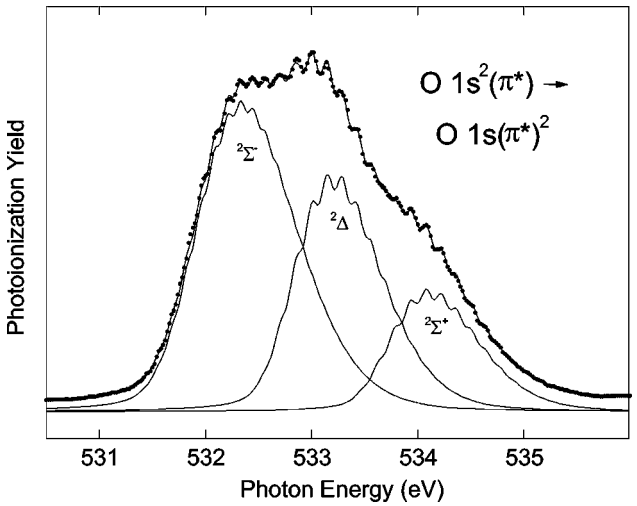

FIG. 3. The O $1s^{-1}\pi^*$ excitation in NO. The solid line through the data points represents the result of a Franck-Condon analysis. The three subspectra describe the three different electronic states.

TABLE V. Results of the Franck-Condon analysis of the O $1s^{-1}\pi^{*2}$ excitations in NO: Given are the vibrational energies $\hbar\omega$, the equilibrium distances r, the energies E, the normalized intensities with respect to the $^2\Sigma^+$ state $f/f(^2\Sigma^+)$, and the lifetime widths Γ for the electronic ground state (g.s.) and the core-excited states $^2\Sigma^-$, $^2\Delta$, and $^2\Sigma^+$. For comparison, the results of Remmers *et al.* [12], the values for the $Z+1$ molecule NF, and the theoretical calculation of Fink [19] are also given. The vibrational energies for the states in the $Z+1$ molecule NF are multiplied with $\sqrt{1.0795}$ according to the different reduced masses. For the energies E, the relative errors are given.

			This work	Remmers *et al.*	NF	Fink
$\hbar\omega$ (meV):	g.s.	235.9				
	$^2\Sigma^-$		137(3)	157(15)	147	139
	$^2\Delta$		154(3)	168(15)	152	159
	$^2\Sigma^+$		157(3)	229(20)	154	162
r (Å):	g.s.	1.151				
	$^2\Sigma^-$		1.348(3)	1.307(7)	1.317	1.339
	$^2\Delta$		1.311(3)	1.283(9)	1.308	1.295
	$^2\Sigma^+$		1.306(3)	1.267(8)	1.300	1.290
E (eV):	$^2\Sigma^-$		531.48(1)	531.46(3)		531.30
	$^2\Delta$		532.60(1)	532.36(3)		532.30
	$^2\Sigma^+$		533.52(1)	533.13(4)		533.38
$f/f(^2\Sigma^+)$:	$^2\Sigma^-$		2.92	1.04		3.52
	$^2\Delta$		1.95	1.14		2.13
	$^2\Sigma^+$		1.00	1.00		1.00
Γ (meV):	$^2\Sigma^-$		170(10)	$\cong$200		174
	$^2\Delta$		170(10)	$\cong$200		175
	$^2\Sigma^+$		170(10)	$\cong$350		173

Fink [19]; all authors agree with the sequence $^2\Sigma^-$, $^2\Delta$, $^2\Sigma^+$. Contrary to previous high-resolution photoabsorption measurements [12,16], the vibrational fine structures of the states are completely resolved and allow a more reliable Franck-Condon analysis. The results of this analysis are represented by the solid line through the data and the three subspectra. The results obtained for the equilibrium distances r', the vibrational energies $\hbar\omega'$, the energies E, the intensity ratios (normalized to the $^2\Sigma^+$ state), and the lifetime width Γ for the core-excited states are summarized in Table V. For comparison, the results of the Franck-Condon analysis performed by Remmers *et al.* [12], the values of the $Z+1$ molecule NF, and the theoretical results obtained by Fink [19] are also given. It can be seen that for all three states, the vibrational energies decrease from $\hbar\omega'=235.9$ meV to $\hbar\omega'\cong150$ meV and the equilibrium distances increase from $r''=1.151$ Å to $r'\cong1.32$ Å . Again, this can be understood by excitation into an antibonding orbital. A more detailed consideration of the O $1s\rightarrow\pi^*$ excitations shows that the equilibrium distance of the $^2\Sigma^-$ state is larger by $\cong30$ mÅ , and the vibrational energy smaller by $\cong20$ meV than for the $^2\Delta$ and $^2\Sigma^+$ states.

The results obtained from the Franck-Condon analysis differ considerably from the values given by Remmers *et al.* [12]. This is especially true for the vibrational energy of the $^2\Sigma^+$ state. The differences can be explained by the fact that a distinct vibrational fine structure is missing in the spectrum of Remmers *et al.*, and that they used the algorithm of Hutchisson [21,22], which is not appropriate to describe transitions with a large number of vibrational substates. Reasonable agreement of the results of the present work with the values for the $Z+1$ molecule is found, especially for the $^2\Delta$ and $^2\Sigma^+$ states; however, the differences for the $^2\Sigma^-$ state are larger. This behavior can be understood on the basis that the energies of the potential-energy surfaces of the states in the core-excited molecule and the $Z+1$ molecule differ by two terms: The first term describes the influence of the different charges of the nuclei in the core-excited and $Z+1$ molecules. This term is equal for all states of the O $1s^{-1}\pi^{*2}$ configuration of NO, and leads to a higher equilibrium distance in the core-excited molecule as compared to the $Z+1$ molecule NF. The second term is the exchange integral K_{xc} between the core hole and the π^* electrons that exist only in NO, but not in the $Z+1$ molecule NF. K_{xc} contributes with a positive sign to the energy of the potential-energy surface of the $^2\Sigma^-$ state, leading to a further increase of the equilibrium distance as compared to the $Z+1$ molecule. However, in the $^2\Delta$ and $^2\Sigma^+$ states K_{xc} with a negative sign leads to a decrease which compensates for the increase caused by the first term. These effects on the geometry of core-excited molecules as compared to the $Z+1$ molecule will be discussed in a more general way elsewhere [37].

The experimental results are also compared with the theoretical calculation of Fink [19]. The experimental vibrational energies were found to be $\cong5$ meV smaller and the equilibrium distances to be slightly larger than the calculated values, as Fink expected on the basis of his calculation. By performing the Franck-Condon analysis, the values of the anharmonicity $x\hbar\omega'$ were kept constant to the values calculated by Fink, with $x\hbar\omega'(^2\Sigma^-)=1.2$ meV, $x\hbar\omega'(^2\Delta)=1.1$

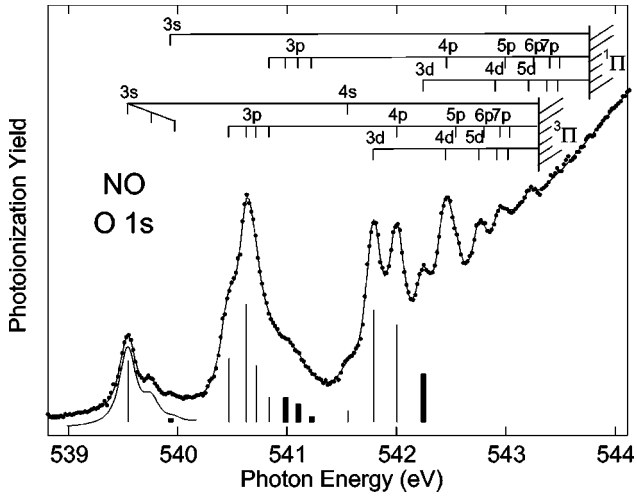

FIG. 4. The Rydberg region of NO below the O 1s ionization threshold. The solid line through the data points represents the result of a fit analysis. The subspectrum below the spectrum describes the result of a Franck-Condon analysis of the O $1s^{-1}3s\sigma$ Rydberg state. The assignments are given by the vertical bar diagrams above the spectrum. The first bar for the 3s resonance represents the $v''=0\rightarrow v'=0$ excitation, while the other bars describe higher vibrational substates. The thin (bold) vertical bars below the spectrum represent the intensities of the weakly overlapping Rydberg states converging toward the $^3\Pi$ ($^1\Pi$) ionization threshold.

meV, and $x\hbar\omega'(^2\Sigma^+)=1.2$ meV; the good fit result of the spectrum with these values indicates that the experimental values should be very similar to the theoretical values. The experimental energies are $\cong$200 meV larger than the calculated values, and the experimental and theoretical intensity distribution (normalized to the $^2\Sigma^+$ state) of the three substates are similar. The experimental and theoretical lifetime widths agree within the errors. Altogether, excellent agreement between the experimental results and the recent calculations by Fink [19] was found.

TABLE VI. The energies E and quantum defects δ of the Rydberg states in NO below the O 1s ionization threshold as obtained from the fit analysis. The relative errors for the energies are estimated to ± 10 meV.

	$^3\Pi$		$^1\Pi$	
	E (eV)	δ	E (eV)	δ
$3s\sigma$	539.540	1.10	539.930	1.11
$4s\sigma$	541.551	1.21		
$3p\pi$	540.463	0.81		
$3p\pi$	540.624	0.74	540.981	0.78
$3p\pi$	540.711	0.70	541.095	0.74
$3p\sigma$	540.933	0.65	541.220	0.68
$4p\pi$	542.000	0.76	542.455	0.76
$5p\pi$	542.539	0.76	542.994	0.76
$6p\pi$	542.800	0.76	543.255	0.76
$5p\pi$	542.946	0.76	543.501	0.76
$6p\pi$	543.035	0.77	543.490	0.78
3d	541.788	-0.01	542.243	0.00
4d	542.447	0.00	542.902	0.00
5d	542.752	0.00	543.207	0.00
6d	542.918	0.00	543.373	0.00
7d	543.018	0.00	543.473	0.00
I_p	543.295		543.751	

C. Rydberg region

The Rydberg region of NO below the O 1s ionization threshold is shown in Fig. 4. The vertical-bar diagrams above the spectrum represent the assignments of the Rydberg states converging toward the O 1s ionization thresholds $^3\Pi$ and $^1\Pi$. This splitting of the thresholds is due to an interaction between the O 1s core hole and the π^* electron. Three Rydberg series with quantum defects of $\delta=1.10$ (ns Rydberg series), $\delta=0.75$ (np), and $\delta=0.00$ (nd) are identified. The energies and quantum defects obtained from the fit analysis are summarized in Table VI. Note that, for NO, similar to CO (see above), a strong mixing between $(n+1)s\sigma$ and $nd\sigma$ Rydberg orbitals (with $n\geqslant 3$) is expected; however, this is of minor importance for the assignment in NO, since no experimental evidence for a splitting of the nd Rydberg states into σ, π, and δ components is found. The assignment given in this work is similar to the results of Remmers *et al.* [12]; however, some previously unobserved resonances were resolved. The improved spectrum allowed determination of the $^3\Pi$-$^1\Pi$ splitting of the O 1s ionization threshold to $\Delta I_p=I_p(^3\Pi)-I_p(^1\Pi)=456(15)$ meV. This value is more precise and significantly smaller than previous results of 510 [12] and 550 meV [38].

The vertical-bar diagram in Fig. 4 represents the intensity of the weakly overlapping Rydberg states. The thin (bold) bars represent the intensity of the states converging toward the $^3\Pi$ ($^1\Pi$) ionization threshold. For the triplet and singlet core-ionized states, an intensity ratio of 3:1 is expected; this also holds for the higher Rydberg states. Contrary to this, the intensity ratio of the two components of the O $1s^{-1}3s\sigma$ state exhibit an intensity ratio of $\cong$15.5:1.

A lifetime width of $\Gamma=150(10)$ meV was obtained for the well-resolved and intense Rydberg states. This value was transferred to the overlapping O $1s^{-1}3p$ states, and made it necessary to describe this part of the spectrum with seven different resonances. This large number of 3p states is due to the interaction of the $nl\pi$ Rydberg states with the π^* electron and the O 1s core hole, and will be discussed in more detail.

By considering the 3p states in a simple way, a symmetry splitting into $3p\sigma$ and $3p\pi$ as well as the splitting of the ionization threshold leads to four different final states; this is not appropriate to describe the measured spectrum, and demonstrates the presence of a more complicated coupling scheme in a convincing way. The coupling scheme given in Table IV results in nine different final states for the O $1s^{-1}3p\pi$ excitations. The six final states with $^2\Sigma^-$, $^2\Delta$, and $^2\Sigma^+$ symmetries are allowed on the basis of selection rules. Therefore, the seven observed structures can only be explained with a symmetry splitting of the 3p states into $p\sigma$ and $p\pi$ components, as well as with a coupling of the $3p\pi$ electron with the electrons in the π^* and O 1s orbitals. An exact assignment of the 3p region on the basis of the present

data is not possible. We, therefore, want to give some arguments and a preliminary assignment.

The observed splitting of $\cong 100$ meV between the different O $1s^{-1}3p$ states is smaller than the $^3\Pi$-$^1\Pi$ splitting of the ionization thresholds of 456(15) meV. It can, therefore, be concluded that the interaction between the core hole and the π^* electron is stronger than the interaction between the $3p$ electron and the core hole or the π^* electron. This is considered in the assignment of the O $1s^{-1}3p$ excitations and, in a first step, the O $1s$ core hole and the π^* electron are coupled to the O $1s^{-1}\pi^*(^{3,1}\Pi)$ core-ionized states. In a second step, the Rydberg electron is coupled with the O $1s^{-1}\pi^*(^{3,1}\Pi)$ ionic states, i.e., we consider the influence of the $3p$ electrons as a small perturbation. This leads to the O $1s^{-1}\pi^*(^{3,1}\Pi)3p\sigma(^2\Pi)$ and O $1s^{-1}\pi^*(^{3,1}\Pi)3p\pi(^2\Sigma^-, {}^2\Delta, {}^2\Sigma^+)$ final states that are allowed on the basis of the selection rules for the spin component of the wave function. In this way the first (last) three observed resonances can be assigned as states converging toward the $^3\Pi$ ($^1\Pi$) ionization threshold. The peak in the middle ($h\nu = 540.933$ eV) cannot clearly be assigned to belong to one specific ionization threshold.

Assuming the interaction of the $3p\pi$ electron with the O $1s^{-1}\pi^*(^{3,1}\Pi)$ configuration to be small is in full agreement with calculations by Kosugi *et al.* [16]. These authors calculated the splitting between the lowest and highest O $1s^{-1}\pi^*(^3\Pi)3p\pi$ and O $1s^{-1}\pi^*(^1\Pi)3p\pi$ state to be 220 and 100 meV, respectively. Due to the distinctly smaller splitting of the O $1s^{-1}\pi^*(^1\Pi)3p\pi$ states, it can be expected that the three components are not completely resolved. The symmetry-resolved photoabsorption spectra of Kosugi *et al.* [16] allow the $nl\sigma$ and $nl\pi$ states to be distinguished, and show that the $3p\pi$ contributions to the spectrum are more intense than the $3p\sigma$ contributions, in agreement with their calculations.

We suggest the following preliminary sequence for the $3p$ states: The first three states are assigned to O $1s^{-1}\pi^*(^3\Pi)3p\pi$, the fourth state to O $1s^{-1}\pi^*(^3\Pi)3p\sigma$, the fifth and sixth state to O $1s^{-1}\pi^*(^1\Pi)3p\pi$, and the seventh state to O $1s^{-1}\pi^*(^1\Pi)3p\sigma$. This assignment results in an intensity ratio for the O $1s^{-1}\pi^*(^3\Pi)3p\pi$ states to the O $1s^{-1}\pi^*(^1\Pi)3p\pi$ states of 5.5:1, which differs distinctly from the expected value of 3:1. The mean energy of the $3p\pi$ states is $\cong 200$ meV lower than of the $3p\sigma$ states; this splitting is twice the calculated splitting of the $3p\sigma/\pi$ splitting in CO below the O $1s^{-1}$ ionization threshold [31].

For a more reliable assignment of the O $1s^{-1}$3p region of the spectrum, further measurements are necessary; e.g., by using high-resolution symmetry-resolved photoionization spectroscopy, which can clearly distinguish between the O $1s^{-1}3p\sigma$ and O $1s^{-1}3p\pi$ states. In principle, this splitting of the O $1s^{-1}nl\pi$ excitations into different states is also present for the higher Rydberg states. However, according to the increase of the distance between the O $1s^{-1}\pi^*(^{3,1}\Pi)$ configuration and the $nl\pi$ electron with increasing n, this splitting becomes smaller and cannot be resolved for the higher Rydberg states.

The vibrational fine structure of the O $1s^{-1}(^3\Pi)3s$ Rydberg state is clearly resolved, and a Franck-Condon analysis is performed, resulting in a decrease of the vibrational energy from $\hbar\omega'' = 235.9$ meV to $\hbar\omega' = 218(2)$ meV, and an increase of the equilibrium distances from $r'' = 1.151$ Å to $r' = 1.190(2)$ Å . The values obtained agree with those of the $Z+1$ molecule NF^+ with $\hbar\omega = 195(5)$ meV and $r = 1.180(6)$ Å [39]. This experimental result on the O $1s^{-1}(^3\Pi)3s$ state in NO is similar to the results in CO at the O $1s$ ionization threshold. It is in agreement with the conclusion of Müller and Ågren [6], and supports the idea of a weakening of the molecular bond upon O $1s^{-1}$ core excitations into Rydberg states or core ionization. This effect can be understood for CO and NO in a simple way using the $Z+1$ approximation, and it will be explained on the basis of the C $1s^{-1}$ and O $1s^{-1}$ core-ionization process in CO: After a C $1s^{-1}$ ionization, CO can be compared with the $Z+1$ molecule NO^+. In NO^+, the difference of the electronegativity of the atoms is smaller than in CO. However, an O $1s^{-1}$ ionization of CO leads to the $Z+1$ molecule CF^+ and a larger difference of the electronegativity of the atoms. This results in a stronger polarization of the valence shell toward the O $1s^{-1}$ or F atom, and a weakening of the multiple bond structure.

For the higher Rydberg states, no vibrational substates were found. This is probably due to the strong overlap of the higher Rydberg states, and may be reinforced by the possibility that vibrational substates for the higher Rydberg states are smaller than for the O $1s^{-1}(^3\Pi)3s$ Rydberg state. This possible effect can be understood by assuming the O $1s^{-1}(^3\Pi)3s$ Rydberg excitation to be a mixed state; it was observed for the O $1s^{-1}3s\sigma$ and O $1s^{-1}3p\pi$ Rydberg states in CO (see above).

V. CONCLUSIONS

The significantly improved energy resolution of the present work allows an experimental observation of the complete vibrational fine structure, and thus Franck-Condon analyses, resulting in detailed information on the potential-energy surfaces, i.e., on the vibrational energies and equilibrium distances of molecules after O $1s$ core excitations. The vibrational fine structure of the O $1s\rightarrow\pi^*$ excitations in CO and NO are completely resolved, allowing Franck-Condon analyses. The values obtained by these analyses are compared with calculations, and reveal good agreement between experiment and theory. For this purpose the spectroscopic parameters for the O $1s\rightarrow\pi^*$ excitations in CO are obtained from accurate *ab initio* calculations. A new assignment is given for the O $1s^{-1}$ Rydberg excitations in CO. The O $1s^{-1}(^3\Pi)3s$ Rydberg state in NO is shown to have a lower vibrational energy and a larger equilibrium distance than the electronic ground state; this supports the idea of a weakening of the molecular bond upon O $1s^{-1}$ excitations.

ACKNOWLEDGMENTS

This work was supported by the Director, Office of Energy Research, Office of Basic Energy Science, Materials Science Division, of the Department of Energy under Contract No. DE-AC03-76SF00098. The work in Berlin was supported by the Bundesminister für Bildung, Wissenschaft, Forschung und Technologie, Project No. 05-SR8KE1-1, and

the Deutsche Forschungsgemeinschaft, Project No. Do-561/1-3. R.F.F. also thanks the Deutsche Forschungsgemeinschaft for support under Contract No. Fi-620/1-2. I.D. and C.C. were partially supported by CONACYT and DGAPA, México. The authors thank T.X. Carroll and T.D. Thomas for providing the computer code that was used to perform Franck-Condon analyses of the O $1s \rightarrow \pi^*$ excitations in CO and NO.

[1] U. Gelius, S. Svensson, H. Siegbahn, E. Basilier, Å. Faxälv, and K. Siegbahn, Chem. Phys. Lett. **28**, 1 (1974).
[2] W. Domcke and L. S. Cederbaum, Chem. Phys. Lett. **31**, 582 (1975).
[3] D. T. Clark and J. Müller, Theor. Chim. Acta **41**, 193 (1976).
[4] D. T. Clark and L. Colling, J. Electron Spectrosc. Relat. Phenom. **12**, 343 (1977).
[5] D. T. Clark and L. Colling, J. Electron Spectrosc. Relat. Phenom. **13**, 317 (1978).
[6] J. Müller and H. Ågren, in *Proceedings of NATO Conference on Molecular Ions*, edited by J. Berkowitz (Plenum, New York, 1983).
[7] R. Püttner, M. Domke, and G. Kaindl, Phys. Rev. A **57**, 297 (1998).
[8] M. Domke, C. Xue, A. Puschmann, T. Mandel, E. Hudson, D. A. Shirley, and G. Kaindl, Chem. Phys. Lett. **173**, 122 (1990).
[9] H. M. Köppe, A. L. D. Kilcoyne, J. Feldhaus, and A. M. Bradshaw, J. Electron Spectrosc. Relat. Phenom. **75**, 97 (1995).
[10] G. Remmers, M. Domke, and G. Kaindl, Phys. Rev. A **47**, 3085 (1993).
[11] H. M. Köppe, B. S. Itchkawitz, A. L. D. Kilcoyne, J. Feldhaus, B. Kempgens, A. Kivimäki, M. Neeb, and A. M. Bradshaw, Phys. Rev. A **53**, 4120 (1996).
[12] G. Remmers, M. Domke, A. Puschmann, T. Mandel, G. Kaindl, E. Hudson, and D. A. Shirley, Chem. Phys. Lett. **214**, 241 (1993).
[13] A. P. Hitchcock and C. H. Brion, J. Electron Spectrosc. Relat. Phenom. **18**, 1 (1980).
[14] Y. Jugnet, F. Himpsel, P. Avouris, and E. E. Koch, Phys. Rev. Lett. **53**, 198 (1984).
[15] G. R. Wight and C. E. Brion, J. Electron Spectrosc. Relat. Phenom. **4**, 313 (1974).
[16] N. Kosugi, J. Adachi, E. Shigemasa, and A. Yagishita, J. Chem. Phys. **97**, 8842 (1992).
[17] B. Kempgens, K. Maier, A. Kivimäki, H. M. Köppe, M. Neeb, M. N. Piancastelli, U. Hergenhahn, and A. M. Bradshaw, J. Phys. B **30**, L741 (1997).
[18] R. Fink, J. Chem. Phys. **106**, 4036 (1997).
[19] R. N. S. Sodhi and C. H. Brion, J. Electron Spectrosc. Relat. Phenom. **34**, 363 (1984).
[20] K. P. Huber and G. Herzberg, *Molecular Spectra and Molecular Structure*, (van Nostrand, New York, 1979), Vol. 4.
[21] E. Hutchisson, Phys. Rev. **36**, 410 (1930).
[22] E. Hutchisson, Phys. Rev. **37**, 45 (1931).
[23] L.-S. Wang, B. Niu, Y. T. Lee, D. A. Shirley, and K. Balasubramanian, J. Chem. Phys. **92**, 899 (1990).
[24] M. Halmann and I. Laulich, J. Chem. Phys. **43**, 438 (1965).
[25] H. A. Ory, A. P. Gittleman, and J. P. Maddox, Astrophys. J. **139**, 346 (1964).
[26] N. Correia, A. Flores-Riveros, H. Ågren, K. Helenelund, L. Asplund, and U. Gelius, J. Chem. Phys. **83**, 2035 (1985).
[27] S. Huzinaga, *Approximate Atomic Functions* (University of Alberta, Edmonton, 1971).
[28] R. Fink and V. Staemmler, Theor. Chim. Acta **87**, 129 (1993).
[29] S. J. Osborne, A. Ausmees, S. Svensson, A. Kivimäki, O.-P. Sairanen, A. Naves de Brito, H. Aksela, and S. Aksela, J. Chem. Phys. **102**, 7317 (1995).
[30] M. Neeb, J. E. Rubensson, M. Biermann, W. Eberhardt, J. Electron Spectrosc. Relat. Phenom. **67**, 261 (1994).
[31] Y. Zhang, P.-H. Zhang, and J.-M. Li, Phys. Rev. A **56**, 1819 (1997).
[32] N. Padial, G. Csanak, B. V. McKoy, and P. W. Langhoff, J. Chem. Phys. **69**, 2992 (1978).
[33] Ch. Jungen, J. Phys. Chem. **53**, 4168 (1970).
[34] K. Kaufmann, J. Phys. B **24**, 2277 (1991).
[35] R. Püttner, M. Domke, K. Schulz, and G. Kaindl, Chem. Phys. Lett. **250**, 145 (1996).
[36] R. Püttner, M. Domke, D. Lentz, and G. Kaindl, Phys. Rev. A **56**, 1228 (1997).
[37] R. F. Fink, R. Püttner, I. Dominguez, T. J. Morgan, C. Cisneros, M. Domke, G. Kaindl, and A. S. Schlachter (unpublished).
[38] D. W. Davis, R. L. Martin, B. S. Banna, and D. A. Shirley, J. Chem. Phys. **59**, 4235 (1973).
[39] *Gmelins Handbook of Inorganic Chemistry, Flourine Supplement*, 8th ed., edited by D. Koschel, P. Kuhn, P. Merlet, S. Ruprecht, and J. Wagner (Springer, Berlin, 1986), Vol. 4, p. 297.